

A new water drive curve at ultra-high water cut stage and application in prediction of oilfield development

Hua Wen¹  · Yikun Liu¹ · Na Sun²

Received: 21 August 2016 / Accepted: 1 November 2016 / Published online: 17 November 2016
© The Author(s) 2016. This article is published with open access at Springerlink.com

Abstract For the water-flooded reservoir at ultra-high water cut stage, the ratio of oil and water relative permeability and the water saturation deviate from the linear relationship and show the downwarping trend in the semi-log coordinate, and the conventional water drive curves show the upwarping trend. Aiming at predicting the dynamic, recoverable reserve and recovery of oilfields at ultra-high water cut stage, a new formula characterizing the relation between the ratio of oil and water relative permeability and the water saturation was proposed, derivation of a new water drive curve was done by reservoir engineering methods, and the formula of recoverable reserve and recovery was derived. Comparison of the new water drive curve and the conventional one through numerical simulation and field application showed higher accuracy and better adaptability resulted from the new water drive curve, which solved the problems of upwarping and big prediction error in curves of ultra-high water cut stage.

Keywords Ultra-high water cut stage · Water drive curve · Relative permeability curves · Recovery · Water cut

Introduction

As a reservoir engineering method for prediction of development index and recoverable reserve, and dynamic analysis in the water-flooded reservoir, the water drive curves play important role in the oilfield development (Chen and Li 2001; Bondar and Blasingame 2002). Since Максимов (1959) from the former Soviet Union firstly put forward the water drive curve in 1959, a lot of effort has been done worldwide in the research on the water drive curve, e.g. Назаров (1972) proposed type D water drive curve in 1972, Tong (1978) introduced the water drive curve proposed by Максимов to China and named it as type A water drive curve in 1978, Сазонов (1973) and Tong (1981) conducted research on type B water drive curve and popularized it in the oilfield development, and Силачев (1981) and Назаров (1982) proposed type C water drive curve. The researchers in China introduced the curves and conducted the theoretical extension and field application (Tong 1989). Chen (1985, 1993, 1994, 1995, 2000) and Yu and Jin (1995), Yu (1999a, 2000) completed theoretical derivation of formulas for type A, B, C, D, and other water drive curves based on oil–water flow in the porous medium. Zhang (1998) completed derivation of water drive curve that is applied widely in the oilfields. Gao and Xu (2007) also conducted theoretical research based on the ratio of oil and water flow in the porous medium. After decades of development, there are more than 50 types of water drive curves (Yu 2000), among which the conventional water drive curves, i.e. type A, B, C, and D ones, are most used in the oilfield development and chosen as four methods in the standard of China’s oil and gas industry (Yu et al. 1999b). The above four methods were derived theoretically based on the rule of flow in the semi-log linear relation between the ratio of oil and water

✉ Hua Wen
wenhuazhg@126.com

¹ College of Petroleum Engineering, Northeast Petroleum University, Daqing 163318, Heilongjiang, China

² Songyuan Gas Recovery Plant, PetroChina Jilin Oilfield Company, Songyuan 138000, Jilin, China

relative permeability and the water saturation in the oil–water relative permeability curves (Chen 2002; Can and Kabir 2014). Field application showed that the linear relation is applicable in the oilfields at medium–high water cut stage. For the oilfields at ultra-high water cut stage, the rule of fluid flow in the formation has been changed fundamentally, and the ratio of oil and water permeability and the water saturation deviate from the linear relationship in the semi-log curve, showing the downwarping trend with nonlinear relation. Correspondingly, the conventional water drive curves are upwarping at ultra-high water cut stage without linear relationship. Thus, the conventional water drive curves are not applicable in the oilfields at ultra-high water cut stage (Chen and Tao 1997). The conventional water drive curves would result in higher recoverable reserve and recovery, creating the big error. Currently, there are few reports about the new formula of the relation between the ratio of oil and water permeability and the water saturation in oilfields at ultra-high water cut stage. Only Liu et al. (2011), Wang et al. (2013), Song et al. (2013), and Cui et al. (2015) in China proposed the exponential and binomial equations for the relation between the ratio of oil and water permeability and the water saturation, completed derivation of exponential, binomial, and inverse-proportion water drive curves, which have some limitations in prediction accuracy. Thus, it needs more effort to work out the water drive curve for the oilfields at ultra-high water cut stage. This paper aims at establishing the new formula of the relation between the ratio of oil and water permeability and the water saturation, based on which the new water drive curve is obtained. The numerical and field application confirmed the applicability of the new water drive curve in prediction of development index, recoverable reserve, and recovery, which is of significance to improvement of evaluation methods of oilfields at ultra-high water cut stage.

New formula of $\ln(K_{ro}/K_{rw})-S_w$ at ultra-high water cut stage

Characteristics of $\ln(K_{ro}/K_{rw})-S_w$ curve

The logarithm of ratio of oil and water relative permeability $\ln(K_{ro}/K_{rw})$ decreases as the water saturation S_w increases. The curve includes three stages: I is the low water cut stage, II is the medium–high water cut stage, and III is the ultra-high water cut stage. At the medium–high water cut stage, $\ln(K_{ro}/K_{rw})$ and S_w show the linear relation, based on which the conventional water drive curves are derived theoretically (Figs. 1, 2). The formula for II linear relation is expressed as (Craig 1971):

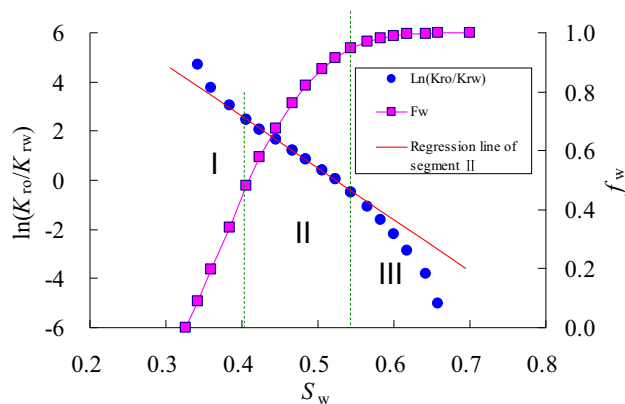


Fig. 1 Curves of oil and water relative permeability

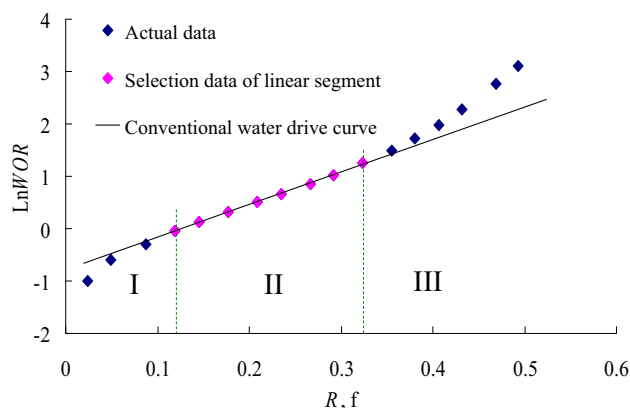


Fig. 2 Water drive curves

$$\ln \frac{K_{ro}}{K_{rw}} = \alpha - \beta S_w \tag{1}$$

namely:

$$\frac{K_{ro}}{K_{rw}} = ne^{-mS_w} \tag{2}$$

where K_{ro} is the oil relative permeability, decimal; K_{rw} is the water relative permeability, decimal; S_w is the water saturation at the outlet, decimal; α and β are the slope and the intercept, respectively; m and n are K_{ro}/K_{rw} and the constant of S_w at the outlet, respectively.

For the oilfields at ultra-high water cut stage, the curves of $\ln(K_{ro}/K_{rw})$ and S_w show the downwarping trend and transform from II linear relationship to III nonlinear relationship, and the water drive curves show the upwarping trend. The main reason is that as the water saturation increases, the oil of continuous phase in the formation transforms to partially continuous phase and non-continuous phase, causing the stronger Jamin effect, substantial reduction in oil permeability, and increment of water permeability, and thus resulting in the downwarping curve of $\ln(K_{ro}/K_{rw})$ and S_w which has the intrinsic rule consistent

with conventional water drive curves showing upwarping trend at ultra-high water cut stage. Application of the conventional water drive curves in analysis of development dynamics of the oilfields at ultra-high water cut stage would result in big error of water cut and higher predicted recoverable reserves. Thus, the formula of $\ln(K_{ro}/K_{rw})$ and S_w characterizing oil and water flow in the oilfields at ultra-high water cut stage is needed to derive the new water drive curve, which is of significance to improvement of the evaluation methods of water-flooded reservoir at ultra-high water cut stage.

New formula of $K_{ro}/K_{rw}-S_w$

Formula (1) describes the typical relation between $\ln(K_{ro}/K_{rw})$ and S_w at the medium-high water cut stage, but it could not be used in the oilfields at ultra-high water cut where $\ln(K_{ro}/K_{rw})$ and S_w deviate from the linear relation. The statistics of relative permeability data from 386 core samples in the Daqing Oilfield showed the obvious non-linearity, e.g. the curve of $\ln(K_{ro}/K_{rw})$ and S_w showed the downwarping trend with water cut between 91 and 93% and inflection points with water cut between 93 and 94%. Normalization of relative permeability data from 15 samples of Nan_1 Block of Sanan Zone in the Daqing Oilfield, 21 samples of Xing_10 of Xingnan Zone, and 17 samples of Xing_5 Block of Xingbei Zone was conducted with average relative permeability method (Table 1), and the curve of K_{ro}/K_{rw} and S_w was plotted (Fig. 3) in the semi-log coordinate by reference to data of oil-water relative permeability of Zhuang_19 Well Block in the Xifeng Oilfield (Song et al. 2013).

It is shown in Fig. 3 that K_{ro}/K_{rw} and S_w in the semi-log coordinate deviate from the linear relation in different degree at ultra-high water cut stage. With statistics of relative permeability data of cores, the formula of $\ln(K_{ro}/K_{rw})$ and S_w at ultra-high water cut stage was derived:

$$\ln \frac{K_{ro}}{K_{rw}} = a + b(S_w - S_{wc}) - c(S_w - S_{wc})^n \tag{3}$$

where $a, b, c,$ and n are constant, which are calculated with the methods in this paper; S_w is the water saturation at the outlet, decimal; S_{wc} is the irreducible water saturation, decimal.

The migration segment with ultra-high water cut in Fig. 3 was fitted using formula (3), which is shown in Fig. 4, and the new formula of K_{ro}/K_{rw} and S_w was obtained through regression, which is shown in Table 2. The above figure and table showed the high precision of formula (3) fitting the relation between $\ln(K_{ro}/K_{rw})$ and S_w at ultra-high water cut stage and confirmed that formula 3 could characterize the relation between K_{ro}/K_{rw} and S_w not only at ultra-high water cut stage but also at the high water cut stage, with more fitted data points and higher

correlation coefficient than the method in reference where the formula is $\ln(K_{ro}/K_{rw}) = -548.1S_w^2 + 639.25S_w - 187.56$ with correlation coefficient of 0.9950 (Song et al. 2013). Thus, formula (3) is applicable in theoretical derivation of new water drive curve and its field application. Moreover, formula 3, which characterizes the relation between K_{ro}/K_{rw} and S_w at ultra-high water cut stage, has higher precision than formula 1 for medium-high water cut stage and the binomial equation of K_{ro}/K_{rw} and S_w for the ultra-high water cut from reference Song et al. (2013).

New water drive curve

Theoretical derivation of formula for new water drive curve

Based on the above formula of $\ln(K_{ro}/K_{rw})$ and S_w for the ultra-high water cut, derivation of corresponding water drive curve was done with the reservoir engineering method (Buckley and Leverett 1942).

According to the relation between the ratio of oil and water relative permeability and the water saturation in formula (3), the following formula was obtained:

$$\frac{K_{rw}}{K_{ro}} = \frac{e^{[-b(S_w - S_{wc}) + c(S_w - S_{wc})^n]}}{e^a} \tag{4}$$

In case of neglecting the gravitational effects and capillary force, the relation between the ratio of oil and water relative permeability and the oil-water production under the steady flow of water flooding is expressed as:

$$\frac{K_{rw}}{K_{ro}} = \frac{Q_w \mu_w B_w \gamma_o}{Q_o \mu_o B_o \gamma_w} \tag{5}$$

$$\frac{Q_w}{Q_o} = \frac{f_w}{1 - f_w} \tag{6}$$

where Q_o is the oil production on the ground, t/d; Q_w is the water production on the ground, t/d; μ_o and μ_w are the oil and water viscosity in the formation, respectively, mPa·s; B_o and B_w are the volume factors of oil and water in the formation, dimensionless; γ_o and γ_w are the relative densities of the degassed oil and the water on the ground, dimensionless; f_w is the water cut, dimensionless.

With formulas (4), (5), and (6), the formula for water-oil ratio WOR is expressed as:

$$\begin{aligned} \text{WOR} &= \frac{f_w}{1 - f_w} = \frac{Q_w}{Q_o} = \frac{\mu_o B_o \gamma_w}{\mu_w B_w \gamma_o} \frac{e^{[-b(S_w - S_{wc}) + c(S_w - S_{wc})^n]}}{e^a} \\ &= \frac{\mu_o B_o \gamma_w}{e^a \mu_w B_w \gamma_o} e^{[-b(S_w - S_{wc}) + c(S_w - S_{wc})^n]} \end{aligned} \tag{7}$$

Logarithm transformation on both sides of formula (7), then:

Table 1 Data of relative permeability from cores of different zones

Sanan			Xingnan			Xingbei			Xifeng (Song et al. 2013)		
Water saturation/f	Relative permeability/f		Water saturation/f	Relative permeability/f		Water saturation/f	Relative permeability/f		Water saturation/f	Relative permeability/f	
	Oil	Water		Oil	Water		Oil	Water		Oil	Water
0.149	1.000	0.000	0.282	1.000	0.000	0.229	1.000	0.000	0.367	1.000	0.000
0.175	0.850	0.008	0.300	0.905	0.005	0.250	0.900	0.005	0.383	0.883	0.054
0.200	0.735	0.015	0.325	0.770	0.015	0.275	0.780	0.015	0.399	0.775	0.072
0.225	0.635	0.024	0.350	0.650	0.025	0.300	0.675	0.020	0.415	0.675	0.086
0.250	0.540	0.030	0.375	0.553	0.034	0.325	0.550	0.030	0.431	0.583	0.098
0.275	0.462	0.038	0.400	0.475	0.040	0.350	0.470	0.040	0.447	0.498	0.108
0.300	0.395	0.046	0.425	0.400	0.049	0.375	0.390	0.051	0.463	0.422	0.117
0.325	0.330	0.055	0.450	0.335	0.056	0.400	0.320	0.065	0.479	0.352	0.125
0.350	0.273	0.060	0.475	0.276	0.065	0.425	0.240	0.075	0.495	0.292	0.132
0.375	0.225	0.066	0.500	0.225	0.075	0.450	0.185	0.095	0.512	0.235	0.139
0.400	0.180	0.075	0.525	0.180	0.085	0.475	0.138	0.115	0.528	0.187	0.145
0.425	0.145	0.084	0.550	0.136	0.095	0.500	0.100	0.138	0.544	0.145	0.151
0.450	0.115	0.094	0.575	0.100	0.107	0.525	0.065	0.165	0.560	0.109	0.157
0.475	0.090	0.107	0.600	0.069	0.120	0.550	0.045	0.195	0.576	0.079	0.163
0.500	0.070	0.123	0.625	0.045	0.135	0.575	0.025	0.240	0.592	0.054	0.168
0.525	0.050	0.142	0.650	0.025	0.150	0.600	0.010	0.285	0.608	0.035	0.173
0.550	0.036	0.166	0.675	0.015	0.165	0.625	0.005	0.345	0.624	0.023	0.178
0.575	0.025	0.192	0.700	0.006	0.184	0.650	0.003	0.415	0.640	0.011	0.183
0.600	0.015	0.225	0.725	0.003	0.200	0.675	0.001	0.500	0.656	0.004	0.187
0.625	0.010	0.270	0.770	0.000	0.235	0.715	0.000	0.635	0.672	0.001	0.192
0.650	0.005	0.315	–	–	–	–	–	–	0.688	0.000	0.196
0.675	0.003	0.370	–	–	–	–	–	–	–	–	–
0.700	0.001	0.425	–	–	–	–	–	–	–	–	–
0.736	0.000	0.500	–	–	–	–	–	–	–	–	–

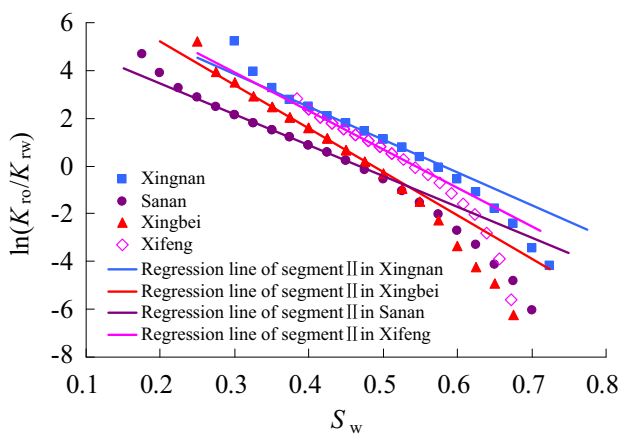


Fig. 3 Curve of K_{ro}/K_{rw} and S_w of cores from different zones

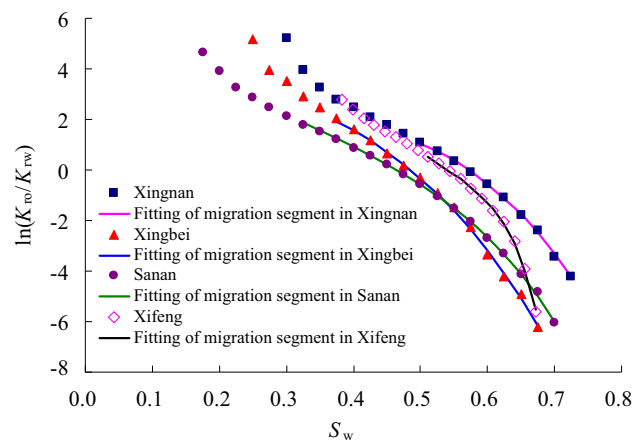


Fig. 4 Fitting of migration segment of $K_{ro}/K_{rw}-S_w$ curve

Table 2 Result of fitting of migration segment of $K_{ro}/K_{rw}-S_w$ curve

Zone	Formula	Correlation coefficient
Sanan	$\ln(K_{ro}/K_{rw}) = 4.0636 - 12.3253(S_w - S_{wc}) - 71.7025(S_w - S_{wc})^{5.1786}$	0.9969
Xingnan	$\ln(K_{ro}/K_{rw}) = 2.5825 - 4.7930(S_w - S_{wc}) - 65.2685(S_w - S_{wc})^{3.2332}$	0.9999
Xingbei	$\ln(K_{ro}/K_{rw}) = 3.5939 - 10.2476(S_w - S_{wc}) - 61.0227(S_w - S_{wc})^{3.0462}$	0.9999
Xifeng	$\ln(K_{ro}/K_{rw}) = 2.8938 - 16.6135(S_w - S_{wc}) - 108167.7(S_w - S_{wc})^{8.7473}$	0.9977

$$\lg \text{WOR} = \lg \frac{\mu_o B_o \gamma_w}{e^a \mu_w B_w \gamma_o} + 0.4343[-b(S_w - S_{wc}) + c(S_w - S_{wc})^n] \quad (8)$$

When the oilfields enter into the high water cut stage, especially the ultra-high water cut stage, the average water saturation in the oil layer is written as (Bondar and Blasingame 2002; Chen and Tao 1997):

$$\bar{S}_w = S_w \quad (9)$$

The accumulative oil production is expressed as:

$$N_p = 100Ah\phi \frac{\gamma_o}{B_{oi}} (\bar{S}_w - S_{wc}) \quad (10)$$

Thus, based on the matter balance equation and formula (10) for the accumulative oil production, the relation between the average water saturation and the recovery per cent is expressed as:

$$\bar{S}_w = \frac{1 - S_{wc}}{N} N_p + S_{wc} = (1 - S_{wc})R + S_{wc} \quad (11)$$

where A is the area of oil reservoir, km^2 ; h is the effective thickness of oil layer, m ; ϕ is the porosity of reservoir; \bar{S}_w and S_{wc} are the average water saturation and the irreducible water saturation, respectively; B_{oi} is the initial volume factor of oil; N is the geological reserve, 10^6t ; N_p is the accumulative oil production, 10^6t ; R is the recovery per cent of oilfield, dimensionless.

Combining formulas (9) and (11) yields:

$$S_w - S_{wc} = \frac{1 - S_{wc}}{N} N_p \quad (12)$$

Substituting formula (12) into formula (8) yields:

$$\begin{aligned} \lg \text{WOR} &= \lg \frac{\mu_o B_o \gamma_w}{e^a \mu_w B_w \gamma_o} + 0.4343 \left\{ -b \frac{1 - S_{wc}}{N} N_p \right. \\ &\quad \left. + c \left[\frac{(1 - S_{wc})}{N} N_p \right]^n \right\} \\ &= \lg \frac{\mu_o B_o \gamma_w}{e^a \mu_w B_w \gamma_o} - 0.4343b \frac{1 - S_{wc}}{N} N_p \\ &\quad + 0.4343c \left(\frac{1 - S_{wc}}{N} \right)^n N_p^n \end{aligned} \quad (13)$$

Define

$$\begin{aligned} A &= \lg \frac{\mu_o B_o \gamma_w}{e^a \mu_w B_w \gamma_o}, \quad B = -0.4343b \frac{1 - S_{wc}}{N}, \\ C &= 0.4343c \left(\frac{1 - S_{wc}}{N} \right)^n \end{aligned} \quad (14)$$

Substituting formula (14) into formula (13), the formula for water drive curve characterizing the oil–water seepage characteristics in the oilfields at ultra-high cut stage is expressed as:

$$\lg \text{WOR} = A + BN_p + CN_p^n \quad (15)$$

Assuming $R = N_p/N$, then the formula between the water–oil ratio (WOR) and the recovery per cent (R) is expressed as:

$$\lg \text{WOR} = A_1 + B_1R + C_1R^n \quad (16)$$

where $A_1 = A$, $B_1 = BN$, $C_1 = CN^n$.

When $n = 1$, formula (15) is transformed into:

$$\lg \text{WOR} = A + (B + C)N_p \quad (17)$$

Defining $B' = B + C$, then

$$\lg \text{WOR} = A + B'N_p \quad (18)$$

Formula (18) characterizes the conventional water drive curve. The new water drive curve is transformed to the conventional one when $n = 1$. The water drive curve derived in this paper integrates the water drive curve at the medium–high water cut stage and that at ultra-high water cut stage, and it is more universal than the conventional one.

When the oilfields reach the abandonment condition, i.e. $f_w = 98\%$, $\text{WOR}_{\max} = 49$, the formula for calculating the recoverable reserve of water-flooded oilfields is obtained with formula (15), then:

$$N_R^n = \frac{1.69 - A - BN_R}{C} \quad (19)$$

The recoverable reserve of water-flooded oilfield N_R in formula (19) is obtained with curve intersection method, and then the recovery of water-flooded oilfield is obtained with $E_R = N_R/N$.

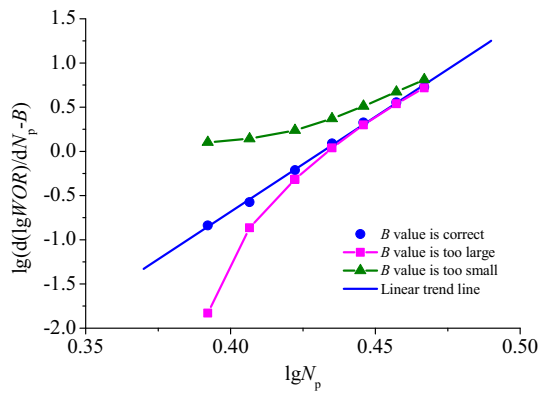


Fig. 5 Parameters determining in new water drive curve by linear trial and error method

Solution to parameters

The new water drive curve is more complex and has more parameters than the conventional one, and it is difficult to calculate the parameters directly. Thus, the parameters of new water drive curves were derived with the new method.

Taking the derivative of the accumulative oil production N_p on both sides of formula (15) yields:

$$\frac{d(\lg WOR)}{dN_p} = B + CnN_p^{n-1} \tag{20}$$

namely

$$\frac{d(\lg WOR)}{dN_p} - B = CnN_p^{n-1} \tag{21}$$

Logarithm transformation on both sides yields:

$$\lg \left[\frac{d(\lg WOR)}{dN_p} - B \right] = \lg Cn + (n - 1) \lg N_p \tag{22}$$

The curve of $\lg \left[\frac{d(\lg WOR)}{dN_p} - B \right] \sim \lg N_p$, which meets the linear relation, was plotted. The value of B was defined with the trial and error method, which is shown in Fig. 5. n , C , and A were obtained according to straight slope, straight intercept, and dynamic data, respectively. The time t_i when the better linear relation exists was chose, then $A_i = (\lg WOR)_{ni} - BN_{pri} - C(N_{pri})^n$. After calculating the values of A_i , the average value $A = \sum_{i=0}^n A_i/n$ with higher precision was calculated. Thus, the parameters in the formula for the new water drive curve were obtained.

Validation and analysis

Validation of numerical simulation

Based on the oil reservoir conditions of Pu_1 Formation of Xing_10 Block of Xingnan Zone in the Daqing Oilfield, the model of five-spot pattern with injector-producer well spacing of 254 m, grid number of $15 \times 15 \times 3$ in IJK direction, and areal mesh size of 24 m was established. The dynamics of oilfields with different ratios of oil and water viscosity were predicted with reservoir numerical simulation, and fitting and comparison of the conventional water drive curve and the new water drive curve were conducted with production data. The fitting result is shown in Fig. 6.

It is shown in Fig. 6 and Table 3 that the conventional water drive curves are applicable only in the linear segment, not in the upwarping segment. The new water drive curve, however, could fit both linear segment and curving segment with correlation coefficient over 0.9976. Moreover, in terms of the recoverable reserve, all the values predicted by the conventional water drive curves are much

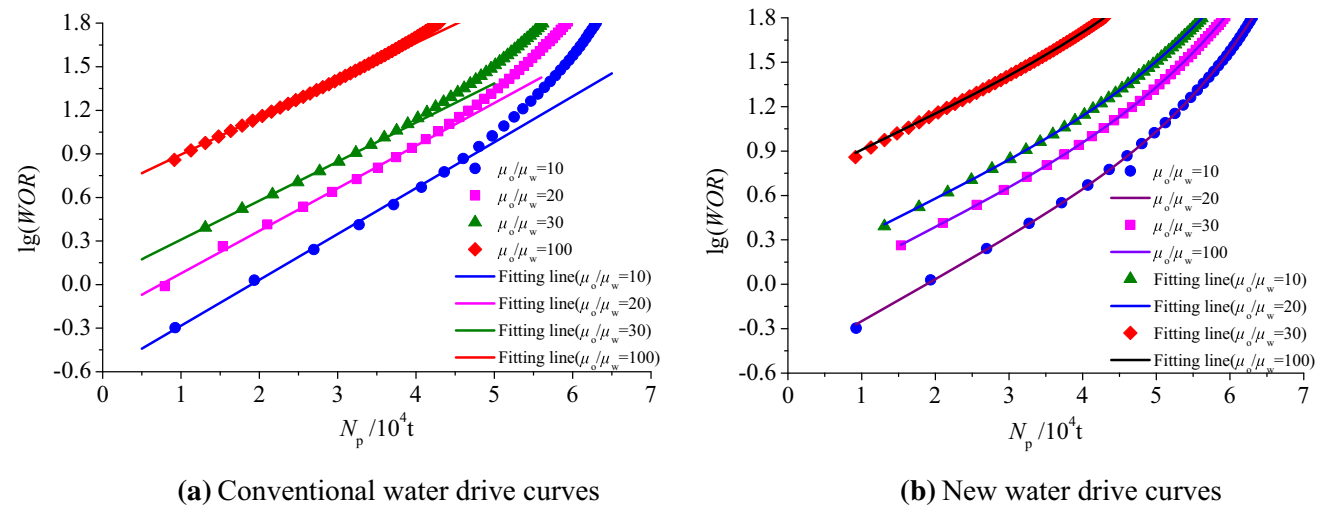


Fig. 6 Comparison of fitting with different water drive curve. **a** Conventional water drive curves, **b** new water drive curves

Table 3 Formula for water drive curves and calculation of recoverable reserve

μ_c/μ_w	The conventional water drive curves			The new water drive curves			Recoverable reserve from numerical simulation/ 10^4t	
	Formula for fitting	Correlation coefficient	Recoverable reserve/ 10^4t	Formula for fitting	Correlation coefficient	Recoverable reserve/ 10^4t	Correlation coefficient	Recoverable reserve/ 10^4t
10	$lgWOR = 0.31592N_p - 0.59967$	0.9974	7.24825	$lgWOR = -0.53449 + 0.28404N_p + 1.6241E-05N_p^{2.65835}$	0.9976	6.1575	0.9976	6.1592
20	$lgWOR = 0.29333N_p - 0.21681$	0.9975	6.50123	$lgWOR = -0.1281 + 0.25665N_p + 6.1028E-05N_p^{4.95327}$	0.9986	5.7304	0.9986	5.7336
30	$lgWOR = 0.26916N_p + 0.03920$	0.9997	6.13388	$lgWOR = 0.07785 + 0.24996N_p + 7.0532E-05N_p^{4.8707}$	0.9996	5.4045	0.9996	5.4041
100	$lgWOR = 0.28367N_p + 0.56848$	0.9999	4.10219	$lgWOR = 0.66715 + 0.2418N_p + 9.4872E-05N_p^{4.75193}$	0.9999	3.9595	0.9999	3.9595

larger than those predicted by numerical simulation, but the value predicted by the new water drive curve is closed to that predicted by numerical simulation with little error. It means that the new water drive curve could fit the data at the high water cut and ultra-high water cut stage with accurate recoverable reserve and has broad adaptability in the oilfields.

Examples

The accuracy and adaptability of the new water drive curve in the oilfields at ultra-high water cut stage were verified with actual data from reference Song et al. (2013), Cui et al. (2015).

Calculation according to Craig FF Jr

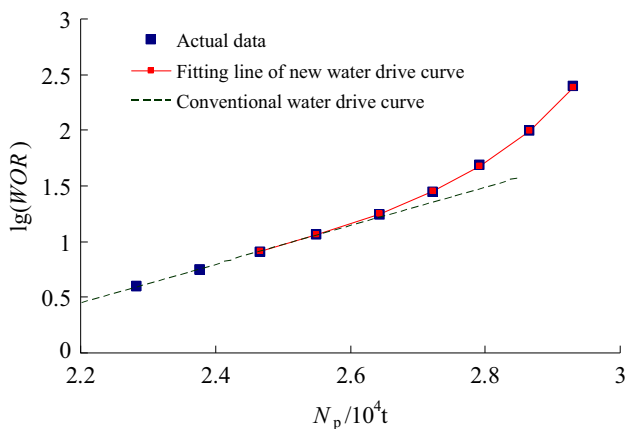
Given reference Craig (1971), Song et al. (2013), the original oil in place is 4.44×10^4t , the initial water saturation is 0.1, the well pattern is the five-spot pattern, and the ratio of oil and water viscosity is 2. The recovery per cent, accumulative oil production, accumulative water production, and other production data corresponding to different water saturation at the outlet are shown in Table 4.

Based on the data in Table 4, the curve of $lgWOR$ and accumulative oil production N_p was plotted with the new water drive curve to compare the new and conventional water drive curves, which are shown in Fig. 7. The front half segment of $lgWOR-N_p$ curve shows the linear relation of the conventional water drive curve, and the latter half segment shows the obvious upwarping trend, which is not the linear relation, and could not be fitted with the conventional water drive curve. Therefore, both front and latter half segments of curve were fitted using new and conventional water drive curves, with which the water-flooded recoverable reserve is predicted for comparison with the results in reference Song et al. (2013) (Table 5).

The fitting results of Fig. 7 show that the latter half segment of $lgWOR-N_p$ curve is well fitted with the new water drive curve with correlation coefficient of 0.9987. The actual water-flooded recoverable reserve resulted from Table 4 is 2.792×10^4t , which is defined as the accumulative oil production with water cut of 0.98, and that calculated by the new water drive curve is 2.7964×10^4t with relative error of merely 0.1576%, which has very high prediction precision. However, the water-flooded recoverable reserve predicted in reference Song et al. (2013) by the water drive curve at ultra-high water cut and the conventional curves has big error, with prediction precision far lower than the methods in this paper. It is believed in reference Song et al. (2013) that the water drive curve of oilfields with high water cut shows the parabola shape.

Table 4 Dynamic data of oilfield

Water saturation at the outlet/f	Water cut/f	Water–oil ratio	Recovery per cent/f	Accumulative oil production/ 10^4 t	Accumulative water production/ 10^4 t
0.469	0.798	3.950	0.514	2.284	0
0.495	0.848	5.579	0.536	2.378	0.523
0.520	0.888	7.928	0.556	2.467	1.227
0.546	0.920	11.500	0.574	2.550	2.191
0.572	0.946	17.518	0.596	2.644	3.833
0.597	0.965	27.571	0.613	2.723	6.009
0.622	0.980	49.000	0.629	2.792	9.394
0.649	0.990	99.000	0.646	2.866	16.719
0.674	0.996	249.000	0.66	2.930	32.688
0.700	1.000	∞	0.667	2.960	

**Fig. 7** Curve of water–oil ratio and accumulative oil production

However, the curve of $\lg WOR - N_p$ is not completely consistent with parabola shape, and the recoverable reserve predicted by binomial water drive curve in reference Song et al. (2013) has big error and is not useful. The comparison of predicted water in Fig. 8 shows that the new water drive curve predicts the water cut more accurately than the conventional one. In conclusion, the new water drive curve

at ultra-high water cut predicts the water-flooded recoverable reserve and water cut more accurately than other water drive curves and has better adaptability.

Example in the Shengli Oilfield

The accuracy and adaptability of the new water drive curve were verified with actual data from reference Cui et al. (2015) (Table 6), which was fitted with the new and conventional water drive curves (Fig. 9). The water-flooded recoverable reserve, which is defined as the accumulative oil production with comprehensive water cut of 0.98, and the water cut were predicted and compared with actual data of oilfields for comparison of the water drive curves in this paper and that in reference Cui et al. (2015).

Based on the data in Table 6, $\lg WOR - N_p$ curve was plotted, and it showed the upwarping trend at ultra-high water cut stage. The parameters of new water drive curve were calculated with formula (22), and the formula of conventional water drive curve was fitted, which is shown in Table 7. It is shown in Fig. 9 that fitting the segment at ultra-high water cut stage in $\lg WOR - N_p$ curve could not be done with the conventional water drive curve, but could be done with the new one proposed in this paper.

Table 5 Prediction of water-flooded recoverable reserve with different water drive curves

Water drive curve		Formula for fitting	Water-flooded recoverable reserve predicted by the water drive curve/ 10^4 t
Reference Song et al. (2013)	Type A	$\lg W_p = -6.3992 + 2.9925N_p$	2.734
	Type B	$\lg WOR = -3.1535 + 1.891N_p$	2.871
	Type C	$L_p/N_p = 0.2576 + 0.3856L_p$	2.727
	Type D	$L_p/N_p = 1.0422 + 0.4124W_p$	2.665
	Binomial method	$\lg WOR = 3.1125N_p^2 - 12.292N_p + 12.98$	2.806
Method derived in this paper		$\lg WOR = -2.86061 + 1.5196N_p + 1.72889E - 10N_p^{20.69277}$	2.7964

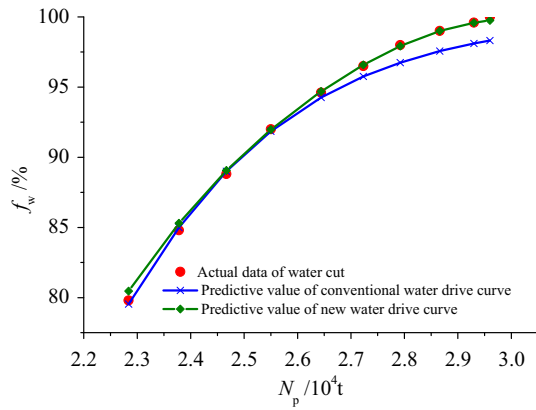


Fig. 8 Curves of water cut predicted by the new water drive curve and the conventional one

With comprehensive water cut of 98%, the water-flooded recoverable reserve predicted by the new water drive curve, the conventional one, and the water drive curve at ultra-high water cut in reference Cui et al. (2015) are $83.9841 \times 10^4\text{t}$, $126.0783 \times 10^4\text{t}$, and $84.80 \times 10^4\text{t}$,

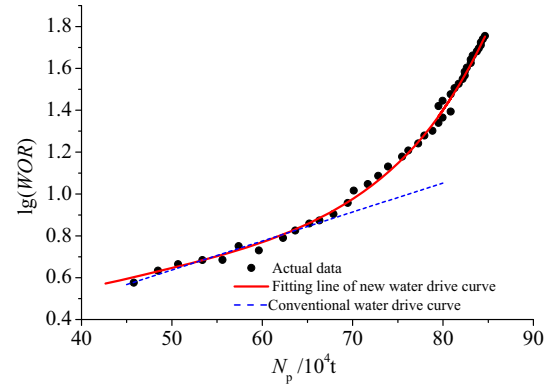


Fig. 9 Comparison of fitting with different water drive curves

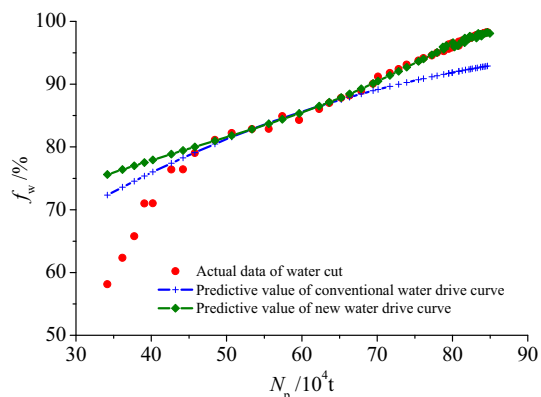
respectively, with error of 0.0166, 50.1465, and 0.988% based on the actual water-flooded recoverable reserve of $83.9702 \times 10^4\text{t}$. Among the water drive curves, the method proposed in reference Cui et al. (2015) has a large disadvantage because S_{or} and S_{wc} depend on other static data and have uncertain value, and it is difficult to work out the formula. Comparison of water cut predicted with the

Table 6 Actual development data in Shengli oilfield

Accumulative oil production/ 10^4t	Water–oil ratio	Water cut/%	Accumulative oil production/ 10^4t	Water–oil ratio	Water cut/%
34.1687	1.39	58.14	76.1538	16.12	94.16
36.1786	1.65	62.33	77.2704	17.43	94.57
37.7419	1.92	65.78	77.9404	19.00	95.00
39.0818	2.45	70.99	78.8337	20.05	95.25
40.1985	2.45	71.04	79.5037	21.88	95.63
42.6550	3.24	76.41	79.9503	23.18	95.86
44.2183	3.24	76.44	80.8436	24.75	96.12
45.7816	3.77	79.03	79.5037	26.32	96.34
48.4615	4.30	81.12	79.9503	27.88	96.54
50.6947	4.62	82.22	80.8436	29.97	96.77
53.3746	4.83	82.84	81.2903	32.06	96.98
55.6079	4.84	82.87	81.7369	33.63	97.11
57.3945	5.63	84.91	82.1836	35.46	97.26
59.6277	5.37	84.31	82.4069	36.76	97.35
62.3076	6.16	86.04	82.4069	38.33	97.46
63.6476	6.69	86.99	82.6302	40.15	97.57
65.2109	7.22	87.83	83.0769	42.24	97.69
66.3275	7.48	88.21	83.0769	43.81	97.77
67.8908	8.01	88.90	83.3002	45.89	97.87
69.4540	9.06	90.06	83.7460	47.98	97.96
70.1240	10.37	91.20	83.9702	49.55	98.02
71.6873	11.15	91.77	84.1935	51.37	98.09
72.8390	12.20	92.42	84.1935	52.94	98.15
73.9206	13.51	93.11	84.4168	55.03	98.22
75.4838	15.08	93.78	84.6400	56.85	98.27

Table 7 Water-flooded recoverable reserve predicted with different water drive curves

Water drive curves	Formula for fitting	Recoverable reserve/ 10^4 t
Conventional water drive curve(type B)	$\lg \text{WOR} = -0.0556 + 0.013847N_p$	126.0783
Reference Cui et al. (2015)	$\lg \text{WOR} = -8.472 + 0.102N_p - 0.09933N_p^2 + 4.581/(1 - S_{or} - S_{wc} - 0.038N_p)$	84.8000
Method derived in this paper	$\lg \text{WOR} = 0.174745 + 0.0092577N_p + 1.37529E-17N_p^{8.6957}$	83.9841

**Fig. 10** Comparison of water cut predicted by different water drive curves

method of water drive curve in Fig. 10 showed that the water cut predicted in this paper is very closed to the actual data. By contrast, the water cut predicted by conventional water drive curve is far less than the actual data, which results in much larger water-flooded recoverable reserve. Obviously, the new water drive curve at ultra-high water cut predicts the water-flooded recoverable reserve and water cut more accurately than other water drive curves and has better adaptability.

Conclusions

- (1) For the oilfields at ultra-high water cut stage, the rule of fluid flow in the formation has been changed fundamentally, and the ratio of oil and water permeability and the water saturation deviate from the linear relationship and show the downwarping trend in the semi-log curve. Thus, the new formula of the ratio of oil and water permeability and the water saturation more applicable in the oilfields was proposed to characterize the curve of K_{ro}/K_{rw} and S_w at ultra-high water cut stage and high water cut stage.
- (2) Based on the new formula of K_{ro}/K_{rw} and S_w at ultra-high water cut stage, the new water drive curve was derived with the reservoir engineering method. The new water drive curve is transformed to the

conventional one when $n = 1$. Comparison of prediction with new water drive curve, conventional one, and methods in references 27 and 28 was done with numerical simulation and field application in two oilfields, which showed that the new water drive curve could fit the development data both at the high water cut and at the ultra-high water cut stage and characterize the upwarping trend at ultra-high water cut stage. The new water drive curve at ultra-high water cut predicts the water-flooded recoverable reserve and water cut more accurately than other water drive curves and has better adaptability.

Acknowledgements This paper is financially supported by the national sci-tech major special project of China (2011ZX05010-002, 2011ZX05052-004, and 2016ZX05010-003), Project of Daqing Oilfield Co., Ltd. (DQYT-0505003-2015-JS-220 and DQYT-0501002-2014-JS-83).

Open Access This article is distributed under the terms of the Creative Commons Attribution 4.0 International License (<http://creativecommons.org/licenses/by/4.0/>), which permits unrestricted use, distribution, and reproduction in any medium, provided you give appropriate credit to the original author(s) and the source, provide a link to the Creative Commons license, and indicate if changes were made.

References

- Bondar VV, Blasingame TA (2002) Analysis and interpretation of water-oil-ratio performance. SPE77569, paper prepared at the SPE annual technical conference and exhibition held in San Antonio, Texas, 29 September–2 October
- Buckley SE, Leverett MC (1942) Mechanism of fluid displacement in sands. Trans AIME 146(1):107–116
- Can B, Kabir CS (2014) Simple tools for forecasting waterflood performance. J Petrol Sci Eng 120:111–118
- Сазонов ВФ (1973) Совершенствование технологии разработки нефтяных месторождений приводонапорном режиме М. Недра
- Chen YQ (1985) Derivation of relationship of water drive curve. Acta Petrolei Sinica 6(2):69–78
- Chen YQ (1993) Derivation of a new type of water displacement curve and its application. Acta Petrolei Sinica 14(2):65–73
- Chen YQ (1994) Classification, correlation and evaluation of water-drive performance curve analysis method. Xinjiang Pet Geol 16(4):348–356

- Chen YQ (1995) Application and derivation of Nazalov's empirical formulas. *Pet Explor Dev* 22(3):63–68
- Chen YQ (2000) Calculation methods of recoverable reserves of oilfields. *Xinjiang Pet Geol* 21(2):130–137
- Chen YQ (2002) Practical methods of petroleum reservoir engineering. Petroleum Industry Press, Beijing, pp 278–410
- Chen YQ, Li D (2001) Modern petroleum reservoir engineering. Petroleum Industry Press, Beijing, pp 148–161
- Chen YQ, Tao ZQ (1997) Derivation of water drive curve at high water-cut stage and its analysis of upwarming problem. *Fault-Block Oil Gas Field* 4(3):19–24
- Craig FF Jr (1971) The reservoir engineering aspects of waterflooding. Society of Petroleum Engineers of AIME, New York, pp 112–114
- Cui CZ, Xu JP, Wang DP, Yang Y, Liu ZH, Huang YS (2015) A new water flooding characteristic curve at ultra-high water cut stage. *Acta Petrolei Sinica* 36(10):1267–1271
- Сипачев НВ, Посевич АГ (1981) Охарактеристиках вытеснения нефти водой. *Нефть и газ* 12:26–32
- Gao WJ, Xu J (2007) Theoretical study on common water-drive characteristic curves. *Acta Petrolei Sinica* 28(3):89–92
- Назаров СН (1972) Коэффициент извлекаемых запасов нефти по интегральным кривым отбора нефти и воды. *АНХ* 5:20–21
- Назаров СН (1982) Исследование Определяющих Параметров Нефтеотдачи. *Известия Высших Учебных Заведений, Нефть, и газ* 6:25–30
- Liu SH, Gu JW, Yang RF (2011) Peculiar water-flooding law during high water-cut stage in oilfield. *J Hydrodyn* 26(6):660–666
- Максимов МИ (1959) Метод подсчета извлекаемых запасов нефти в конечной стадии эксплуатации нефтяных пластов в условиях вытеснения нефти водой. *Геология нефти и газа* 42(3):42–47
- Song ZJ, Li ZP, Lai FP, Liu G, Gan HH (2013) Derivation of water flooding characteristic curve for high water-cut oilfields. *Pet Explor Dev* 40(2):201–208
- Tong XZ (1978) Study on statistical characteristics of natural water flooding and artificial water flooding reservoir. *Pet Explor Dev* 4(6):58–64
- Tong XZ (1981) Analysis of well production and reservoir dynamics. Petroleum Industry Press, Beijing, pp 37–60
- Tong XZ (1989) Application of Tong's water flooding curve analysis method to analyzing some reservoir performance problems in the world. *Pet Explor Dev* 10(3):41–49
- Wang RR, Hou J, Li ZQ (2013) A new water displacement curve for the high water-cut stage. *Pet Sci Technol* 31(13):1327–1334
- Yu QT (1999a) Characteristic of oil-water seepage flow for several important water drive curves. *Acta Petrolei Sinica* 20(1):56–60
- Yu QT (1999b) Study on water displacement curve—The 6th in Series. *Xinjiang Pet Geol* 20(2):141–145
- Yu QT (2000) A generalized water displacement curve of forecasting oilfield development indexes. *SPE* 64717
- Yu QT, Jin HW (1995) Generalized water displacement curve. *Acta Petrolei Sinica* 16(1):61–69
- Zhang JQ (1998) A new practical water displacement curve. *Pet Explor Dev* 25(3):56–57